



Effect of Carbonic Maceration (CM) on the Vacuum Microwave Drying of Chinese Ginger (*Zingiber officinale* Roscoe) Slices: Drying Characteristic, Moisture Migration, Antioxidant Activity, and Microstructure

Kejing An¹ · Lai Wei¹ · Manqin Fu¹ · Lina Cheng¹ · Jian Peng¹ · Jijun Wu¹

Received: 27 January 2020 / Accepted: 23 July 2020 / Published online: 30 July 2020
© Springer Science+Business Media, LLC, part of Springer Nature 2020

Abstract

Ginger is an important Chinese flavoring agent and a traditional herbal medicine. Traditional drying method for ginger may cause severe damage and destroy the chemical and physical qualities. Carbonic maceration (CM) is an efficient and low-cost technology, which can increase the mass transfer rate during drying process and improve the quality indices of ginger. The results showed that CM treatment could produce porous structure and increase the cell membrane permeability, which significantly increases the moisture diffusion and evaporation rate, especially the internal moisture diffusion. The total drying time can be shortened by $42.27 \pm 2.78\%$. Due to the increase of cell membrane permeability, the plant extraction barrier was decreased; thus, the extracted active components were enhanced. Besides, the lower pH environment and inactivation of polyphenol oxidase (PPO) and peroxidase (POD) were also beneficial to increasing the phenol compound retention as well as antioxidant activities. The contents of 6-gingerol, 8-gingerol, 10-gingerol, and 6-shogaol were increased by 20.79%, 37.27%, 36.80%, and 68.53% respectively after CM treatment. The 2,2-diphenyl-1-picrylhydrazyl, ferric-reducing antioxidant power, and oxygen radical absorption capacity values were also increased by 1.33, 1.28, and 1.20 times respectively. Therefore, CM pretreatment could be a suitable alternative technique for improving drying characteristics and preserving nutritional values of agro-based product.

Keywords Low-field nuclear magnetic resonance (LF-NMR) · PPO and POD activity · Circular dichroism analysis · Gingerols · Antioxidant activity

Chemical Compounds Studied in This Article 6-Gingerol (PubChem CID: 442793)

8-Gingerol (PubChem CID: 168114)

10-Gingerol (PubChem CID: 168115)

6-Shogaol (PubChem CID: 5281794)

Zingerone (PubChem CID: 31211)

2,2-Diphenyl-1-picrylhydrazyl (PubChem CID: 74358)

Trolox (PubChem CID: 40634)

TPTZ (2,4,6-tripyridyl-s-triazine) (PubChem CID: 77258)

2, 2'-Azobis (2-amidino-propane) dihydrochloride (PubChem CID: 76344)

Gallic acid (PubChem CID: 370)

Electronic supplementary material The online version of this article (<https://doi.org/10.1007/s11947-020-02504-y>) contains supplementary material, which is available to authorized users.

✉ Jijun Wu
wujijun@gdaas.cn

Kejing An
ankejing2008@163.com

¹ Sericultural & Agri-Food Research Institute, Guangdong Academy of Agricultural Sciences/Key Laboratory of Functional Foods, Ministry of Agriculture and Rural Affairs/Guangdong Key Laboratory of Agricultural Products Processing, Dong Guanzhuang Yiheng RD., Tianhe District, Guangzhou 510610, People's Republic of China

Introduction

Ginger (*Zingiber officinale* Roscoe), a plant which belongs to the Zingiberaceae family, has been widely used as a spice or a common condiment for a variety of compounded foods (Larsen et al. 1999). It is also an important medicine for treating cold, stomach upset, diarrhea, and nausea. Phytochemical studies show that ginger has antioxidant, anti-inflammatory, and cancer preventive activities (Shukla and Singh 2007). The characteristic components of ginger include essential oil and oleoresin. The essential oil, which is a mixture of monoterpenic and sesquiterpenic compounds, is responsible for the characteristic ginger flavor. The oleoresin contains the substances responsible for the pungent flavor of fresh ginger, which are phenolic ketones, known as 4-, 6-, 8-, 10-, and 12-gingerol. Nevertheless, during storage or thermal processing, the gingerols may be modified to a series of homologous compounds called shogaols. Studies have proved that shogaols are more pungent, and exhibit higher antioxidant activity than gingerols (Guo et al. 2014).

Fresh gingers usually contain 85–95% water and are susceptible to microbial spoilage and chemical deterioration (Mishra et al. 2004). Drying is one of the most practiced processing procedures in food industry as it is an effective way for inhibiting microbial growth, delaying deteriorative biochemical reactions, and minimizing the packing, storage, and transportation cost (Esturk 2012; Doymaz 2007). It is also a fundamental processing method to achieve new products. Dried ginger can be utilized for manufacturing of ginger spices, medicines, and essential oil which can be added in cosmetics, soft drinks, and candies. However, at present, the research on ginger drying process is very primary in China, neither a comprehensive study of suitable ginger drying technology, nor complete technical parameters. The traditional ginger drying method mostly uses coking coal as fuel or natural air drying. These drying methods will lead to high sulfur content of ginger, poor product quality, easily polluted by mold, and other problems, which are restricted by environmental protection and international market export. Therefore, whether we can find a low energy consumption, high quality, high efficiency, and pollution-free drying technology has become the focus of the ginger industry in recent years.

Vacuum microwave drying (MVD) is a drying method developed on the basis of microwave and vacuum technology. It has the characteristics of fast drying speed, low drying temperature, and oxygen isolation. However, high energy consumption and uneven microwave heating are the main bottlenecks restricting the application of MVD. As the drying proceeds, the internal temperature of the material is significantly higher than the external, and the dense pore structure is gradually formed inside the material, which leads to poor thermal conductivity and uneven heating of the material. Therefore, it is necessary to find a pretreatment to modify the micropore

structure, enhance the cell permeability and thermal conductivity of the material, and thus improve the mass and heat transfer performance during drying as well as quality attributes of the final products.

Many pretreatments have been reported to shorten drying time, reduce energy consumption, and improve quality attributes, such as chemical dipping (sodium hydroxide, potassium carbonate, methyl and ethyl ester emulsions) (Doymaz 2006), thermal treatment (Tarhan 2007), and high-pulsed electric field (HPEF) (Taiwo et al. 2002). However, chemical dipping could overcome the wax barrier, and has no significant effect on dense flesh (Bain and McBean 1969). Thermal treatment could cause substantial wastewater disposal. As for HPEF treatment, the equipment is still too expensive and complicated to employ at the moment. Therefore, a new pretreatment named carbonic maceration was introduced, which is low cost, efficient, and has easy operation.

Carbonic maceration (CM) was first invented by Michael Flanzy in 1934 and had been used in grape making to improve the aroma of final products (Tesniere and Flanzy 2011). Since CM process could result in structure changes of grape, such as collapse of cell wall and hydrolysis of cell membrane, and induce some physiochemical reactions in the vacuole, this technique was recently studied as a pretreatment before drying of many fruits and vegetables. Tao (2013) reported after CM treatment that the air drying and infrared drying of red raisin were shortened by 65.15% and 71.95%. Liu et al. (2014) found CM treatment could improve the microwave drying rate of chili by 1.5–1.85 times, and the TPC and Vc contents were also increased by 40–60% and 121–582%, respectively. Liu and Wang (2011) found CM treatment prior to drying could increase the total phenolic (TPC) and ascorbic acid (Vc) content of grape by 41.28% and 12.81%. These studies demonstrated that CM pretreatment could accelerate the drying process as well as preserve better nutritional values. As a follow-up study, we have conducted a thorough study to explore the effect of CM pretreatments on the changes of microstructure, water migration, and mechanism of CM pretreatment.

Thus, the main objectives of the current study are to (1) evaluate the effect of CM pretreatment on the vacuum microwave drying characteristics, water migration, and microstructure changes of ginger slices; (2) investigate the impact of CM pretreatment on the quality attributes of dried ginger slices; and (3) explore the mechanism of CM pretreatment on ginger slices

Materials and Methods

Reagent and Chemicals

Acetonitrile and methanol (HPLC grade) were purchased from Honeywell (Morris, N.J, USA). Authentic standards of

6-, 8-, 10-gingerol, and 6-shogaol were purchased from Mansite Biotechnology Co., Ltd. (Chengdu, China). Folin-Ciocalteu reagent, 2,2-diphenyl-1-picrylhydrazyl (DPPH), and ethylenediaminetetraacetic acid (EDTA) were from Yuanye Bio-Technology Co., Ltd. (Shanghai, China). Total ferric-reducing antioxidant power (FRAP) and oxygen radical absorption capacity (ORAC) assay kit were purchased from Nanjing Jiancheng Biotechnology Research Institute (Nanjing, China). Other reagents, methanol, ethanol, sodium carbonate anhydrous, ethyl acetate, ascorbic acid, sodium hydroxide, glacial acetic acid, gallic acid, guaiacol, catechol, PVPP, PEG 6000, and Trolox, were from National Pharmaceutical Corporation (Beijing, China).

Material

The fresh matured gingers (Shandong Laiwu variety) were bought from a local market in August, 2018. Raw ginger rhizomes were washed thoroughly for a short time and blotted up with filter paper to remove the excess water. Gingers were then cut into cylinder slices with thickness of 4 ± 0.2 mm and diameter of 34 ± 2.0 mm. The initial moisture was determined by using a vacuum oven at 70°C with 13.3 kPa, until the weight of samples was constant. Gingers used for experiment were from the same batch.

Carbonic Maceration

CM experiment was conducted in a laboratory set-up equipment, and the schematic diagram was shown in Supplementary Fig. 1. Ginger slices were weighed and placed into the tank, and then the tank was filled with CO_2 to desired pressures and heated to certain temperature. After a period of CM treatment for certain temperature and pressure, gingers were taken out, and gently blotted with tissue paper and weighed. The preliminary experiments showed that CM1 (2 MPa-3 h- 40°C), CM2 (1 MPa-3 h- 45°C), and CM3 (2 MPa-5 h- 45°C) were the optimum CM conditions (Wei et al. 2019). Therefore, these three conditions were adopted for further study.

Drying Process of Ginger Slices

A total of 100 g ginger slices was put into the laboratory model vacuum microwave dryer (RX-10ZK, Guangzhou Rongxing Industrial Microwave Equipment Co., Ltd., China) with an output of 1200 W and vacuum degree of -90 kPa, including a control unit for microwave pulse ratio (PR) regulation. The optimized condition of vacuum microwave drying: initial drying stage of PR was 1.7 (10 s on-7 s off) until 30% w.b., then changed to the second stage PR of 3.0 (5 s on-10 s off) to the end of drying (Supplementary

Table 1). When moisture content reached to $12.0 \pm 2.0\%$, the drying process ended.

Moisture Ratio and Drying Rate

Moisture ratio (MR) and drying rate (DR) can be expressed as follows (Thakor et al. 1999):

$$\text{MR} = \frac{M - M_e}{M_0 - M_e} \quad (1)$$

$$\text{DR} = -\frac{dM}{dt} = -\frac{M_{d,i+1} - M_{d,i}}{t_{i+1} - t_i} \quad (2)$$

where M is the instantaneous moisture content, dry basis; M_0 is the initial moisture content, dry basis; M_e is the equilibrium moisture content, which can be assumed as zero when compared with M_0 . $M_{d,i}$, $M_{d,i+1}$ is the moisture content at time t_i , t_{i+1} , dry basis.

NMR and MRI analysis

The water status of the fresh and CM pretreated ginger samples was determined by nuclear magnetic resonance (NMR) and magnetic resonance imaging (MRI) analysis as described by Wang et al. (2018). Approximately 5 g of ginger slices was placed inside a 25-mm glass tube and inserted in a low-field pulsed NMR analysis (PQ001, Niumag Electric Corporation, Shanghai, China). The height of measurements was controlled in 20 mm. Carr-Purcell-Meiboom-Gill (CPMG) sequences were used to measure the spin-spin relaxation time (T_2). Optimal pulse parameters were $P1 = 6 \mu\text{s}$, $SF = 20$ kHz, $SW = 100$ kHz, $TD = 700,028$, $DR = 1$, $DRG1 = 3$, $TW = 1500,000$ ms, $NS = 4$, and $NECH = 7000$. Each measurement was performed in triplicate.

The 2D proton density images from transverse section of fresh and CM pretreated ginger samples were analyzed by the MRI. Typical pulse parameters were as follows: $TE = 20$ ms, $TR = 500$ ms, matrix size = 256×256 , $FOV = 100 \times 100$ mm, slice width = 2.6 mm, and slices = 3.

Microstructure of Dried Ginger

Microstructure changes of dried ginger slices with different pretreatments were analyzed using a scanning electron microscope (Phenom-World BV, Eindhoven, The Netherlands). To obtain the SEM images, $5 \times 5 \times 5$ mm³ small pieces were taken from both the inner and surface parts of dried ginger slices, then glued on the metal stub. Each specimen was coated with a very thin layer of gold under high vacuum and analyzed by a scanning electron microscope.

Color Measurements

Color of ginger slices was measured using a Lab-scan colorimeter (MS/S-4500 L; Hunter Associate Laboratory Inc., VA, USA). In the measurement, the reflection mode was chosen, and after calibration, the samples were put into the instrument and multiple measurements were performed on different parts of the same dried ginger slice. The L^* value is a measure of lightness, ranging from 0 (black) to + 100 (white); a^* value ranges from – 100 (greenness) to + 100 (redness) and b^* value ranges from – 100 (blue) to + 100 (yellowness). The total color difference (ΔE^*) was determined by using the following equation (Romano et al. 2008):

$$\Delta E^* = \sqrt{[(L^* - L_0^*) + (a^* - a_0^*) + (b^* - b_0^*)]^2} \quad (3)$$

where L_0^* , a_0^* , and b_0^* refer to the color of fresh ginger before drying, while L^* , a^* , and b^* are color values after drying.

Determination of 6, 8, 10-gingerol, and 6-shogaol by HPLC Method

Extracts were prepared according to the procedure described by Chan et al. (2008). Dried ginger slices were grounded into powder and sieved with 60-mesh wire screens and 5 g of the ginger powder was accurately weighed and placed into a beaker; then, 30 ml of 80% aqueous methanol was added. Beaker was ultrasonically extracted three times for 30 min each time and filtered. Methanol was removed by drying at 40 °C in a rotary evaporator. After concentrating, the extract was transferred to a 50-ml volumetric flask and made up to the volume. The solution was filtered through a 0.45- μ m organic membrane filter to an auto sampler vial for HPLC analysis. The extraction procedure was repeated.

The chromatographic separation was carried out using the LC-20A HPLC system (Shimadzu Co., Japan) according to the method of Cheng et al. (2011). It was performed on a Sunfire™ C₁₈ column (4.6 × 250 mm i.d., 5 μ m). The mobile phase was prepared from water (A) and acetonitrile (B). The gradient program for the HPLC was as follows: 0–5 min, 0–5%B; 5–25 min, 5–25%B; 25–30 min, 25–35%B; 30–50 min, 35–60%B; and 51 min, 60–5%B. The flow rate was 1 ml min⁻¹, the injection volume was 20 μ l, and the column temperature was maintained at 30 °C. The detection wave length was set at 280 nm.

Determination of Total Phenolic Content and Antioxidant Activity

Total phenolic content (TPC) of ginger was determined using the Folin-Ciocalteu assay according to Singleton et al. (1999).

Ginger extracts (400 μ l) were introduced into test tubes followed by 2.0 ml of Folin-Ciocalteu phenol reagents (10 times dilution with deionized water). After 5 min, 3.0 ml of sodium carbonate (7.5% w/v) solution was added to the mixture. The absorbance was measured at 765 nm using a spectrophotometer (UV-726, Shimadzu, Shanghai, China) after 2 h reaction in darkness. A total of 80% methanol was taken as blank. The amount of total phenolics was expressed as gallic acid equivalents (GAE, mg/g of dry sample).

DPPH radical scavenging assay is based on the measurement of the scavenging ability of antioxidants toward the stable DPPH radical. It was conducted according to Lim and Murtijaya (2007) with modifications. Different dilutions of extract (0.4 ml) were added to 3.5 ml of 0.14 m mol/l DPPH solution in methanol and shaken vigorously. The mixture was allowed to stand for 30 min before measuring the absorbance at 517 nm. Results were also expressed as IC₅₀ and ascorbic acid equivalent antioxidant capacity (AEAC). IC₅₀ of the extract was determined from the graph of antioxidant activity (%) against amount of extract (mg). Antioxidant activity was expressed using the equation:

$$AA\% = [(Abs_{control} - Abs_{sample})/Abs_{control}] \times 100 \quad (3)$$

where control: 3.5 ml, 0.14 mM, DPPH, +0.4 ml, 80% methanol; sample: 3.5 ml, 0.14 Mm, DPPH, +0.4 ml extract.

For ferric-reducing antioxidant power (FRAP) method, the total antioxidant capacity is expressed with the concentration of FeSO₄ standard solution. 27.8 mg FeSO₄·7H₂O was accurately weighed and dissolved in 100 ml water to 1 mmol/l, diluted the standard solution to 0.1, 0.2, 0.4, 0.6, 0.8, and 1.0 mmol/l, respectively, mixed the test buffer, matrix solution, and substrate solution in the kit in the proportion of 10:1:1, and then incubated at 37 °C in the dark.

Determination of total antioxidant capacity took 5 μ l ginger extract and drop it into 96 pore plates one by one, then added 180 μ l working solution into each pore and incubated at 37 °C in the dark for 3–4 min. Multi-functional microplate reader (BioRad550, BioRad, USA) was used to read the absorbance value at 593 nm. Distilled water was used as blank, and FeSO₄·7H₂O solutions were used to set standard curve.

The oxygen radical absorption capacity (ORAC) assay was performed using an automated plate reader (BioRad550, BioRad, USA) according to the method of Wolfe et al. (2008). The ginger extract (20 μ l) was placed in each microplate well. This was followed by addition of 80 μ l of a sodium fluorescein solution (1.25 μ mol/l in 75 mmol/l phosphate buffer, pH 7.4) into each well and then incubation for 5 min at 37 °C. Then, 100 μ l of freshly prepared AAPH (140 mmol/l in 75 mmol/l phosphate buffer, pH 7.4) was added to each well. Excitation and emission spectra were recorded at 485 and 520 nm, respectively, every 2.5 min for 35 cycles at 37 °C. The ORAC results were expressed as Trolox equivalent (TE).

PPO and POD Activity Measurement

The enzyme extracts were made by homogenization of 5 g of each sample with 5 ml of 0.1 M acetate buffer (pH 5.5) (containing 4% (w/v) PVPP and 340% (w/w) PEG 6000). The PPO activity was assayed using 0.1 ml extract and 4.0 ml of a solution with 0.15 M catechol in 0.05 M acetate buffer (pH 5.5). The reaction was measured at 420 nm and 25 °C. The POD activity was assayed using 0.5 ml extract and a reaction mixture composed of 25 mmol of guaiacol (50 mmol/l acetate buffer, pH 5.5) with 200 µl and 0.5 mol/L H₂O₂. The oxidation of guaiacol was measured at 470 nm and 25 °C. Enzyme activity unit was defined as an increase of 0.1 in absorbance per minute. Residual activity (RA) of enzyme was defined as:

$$RA = \frac{\text{enzyme activity after CM treatment, } A_t}{\text{initial enzyme activity, } A_0} \quad (4)$$

Circular Dichroism Analysis of PPO and POD

Circular dichroism (CD) spectra were recorded with Chirascan™ systems (Applied Photophysics Ltd., UK), using quartz cuvette of 1-mm optical path length at room temperature (25 ± 1 °C). CD spectra were scanned at the far UV range (260–200 nm) with four replicates at 50 nm/min, bandwidth = 1 nm. The contents of α-helix (%), β-sheet (%), β-turn (%), and Rndm.coil (%) were analyzed by the CDNN software (Leatherhead, UK).

Fluorescence Spectroscopy Analysis

Fluorescence spectra were measured with a HITACHI F-4500 spectrofluorometer (HITACHI, Japan), using quartz cuvette of 1-cm optical path length at room temperature (25 ± 1) °C. The emission spectra (λ_{em}: 300–400 nm) were obtained at the maximum excitation wavelength (λ_{ex}: 280 nm for PPO and 270 nm for POD) and represented the mean of four scans. The result can be expressed by relative fluorescence intensity (RFI)

$$RFI = \frac{\text{fluorescence intensity after CM treatment}}{\text{fluorescence intensity before CM treatment}} \times 100\% \quad (5)$$

Cell Membrane Permeability

Cell membrane permeability was estimated by relative electrolyte leakage (REL) according to Galindo et al. (2005). Ginger slices were put into deionized water

and treated under vacuum condition for 10 min, then shaken (120 rpm) for 1 h. The electrical conductivity was measured using a conductivity meter (CPC-505, smarttester, Germany) to determine electrolyte leakage. Tissues were later destroyed by heating in boiling water for 10 min. After cooling, the conductivity of the bathing medium was measured. REL was calculated as the ratio of conductivity before and after tissue destruction.

Statistical Analysis

The results were analyzed using one-way analysis of variance (ANOVA) and Duncan's multiple-range test ($P < 0.05$), carried out with SPSS 18.0 (Chicago, IL, USA). All experiments were run in triplicate.

Results and Discussion

The Effect of CM Pretreatments on Drying Characteristics of Ginger Slices

Moisture ratio (MR) curves were observed to be reduced exponentially with drying time (Fig. 1a). Curves which exhibited steeper slope had higher drying rate. As shown in Fig. 1a, the curve of CM3 (2 MPa-5 h-45 °C) showed the steepest slope, followed by CM2 (1 MPa-3 h-45 °C), CM1 (2 MPa-3 h-40 °C), and fresh samples. Though the moisture ratio of fresh samples declined faster in the beginning of drying, it did slower in the later stage of drying, compared with CM samples. Therefore, the fresh samples need much longer time than the CM samples to reach the final moisture content (Fig. 1a).

The drying rate curves echoed this result. In vacuum microwave drying of ginger, the drying rate curves can be generally identified in two distinct periods: warming up and falling rate periods (Fig. 1b), which was consistent with many previous studies (Fig. 2009, 2010; Chong et al. 2013). After CM treatments, the drying rate of ginger was significantly increased, especially in the falling rate period (Fig. 1b). According to Azzouz et al. (2002), the drying efficiency depends on the nature of the material and difficulty of capillary diffusion. When plant tissue was put in a low pH environment, depolymerization of pectin and other connecting biopolymers occurred. The hydrolysis of cell wall and increase in cell membrane permeability could considerably reduce the mass transfer resistance and increase the drying rate (Krall and McFeeters 1998). CM pretreatments can create an acidic environment, which help to hydrolyze glycoside bond of ginger and induce micro-channels of ginger and thus the drying rate of ginger after CM was increased. As shown in Fig. 1b, the

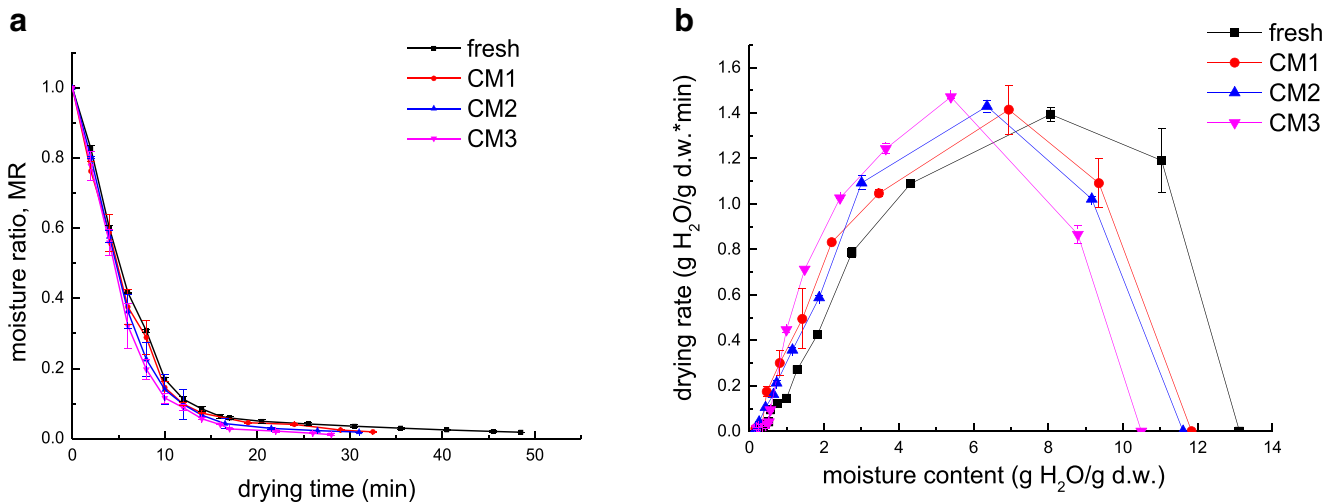


Fig. 1 The curves of moisture ratio (a) and drying rate (b) of vacuum microwave drying of ginger after CM treatments

CM3 samples showed the highest drying rate, whose drying time was 42.27% less than untreated samples.

Effect of CM Pretreatments on the Water Status of Ginger Slices

To investigate the status of water molecules of ginger slices after CM pretreatment, the analyses of spin-spin relaxation times (T_2) by LF-NMR and MRI image were carried out. As shown in Fig. 2, the distribution of T_2 relaxation times in ginger slices with and without CM pretreatment showed three population groups of protons: T_{21} (0.01–10 ms), T_{22} (10–100 ms), and T_{23} (100–1000 ms). According to Xu et al. (2015), the higher T_2 relaxation time is consistent with the weaker degree of bound hydrogen proton or the greater freedom degree of hydrogen. The region T_{21} ascribes to the water molecules (hydration monolayer water) bound by strong H-bonds, which is associated with the water contained in cell walls. The

region T_{22} represents the water molecules (multilayer water) strongly bound to the monolayer, which is related to the water contained in cytoplasm and extracellular. The region T_{23} stands for the water molecules (“free” or solvent water) weakly bound to the product, which is relevant to the water contained in the vacuole. As can be seen from Fig. 3, the curve of the pretreated samples at the beginning of drying shifted toward the left of the X axis compared with the fresh samples while the curves of the pretreated samples during the drying process (2–30 min) shifted toward the right of the X axis compared with the fresh samples at the same drying time. This is because CM treatment could remove part of free water from fresh ginger before drying. Besides, CM could also induce micro-channels of ginger, reduce water bound ability, and improve hydrogen proton freedom; thus, bound water is decreased and transforms into free water (Turgut et al. 2018).

The relative areas of T_{21} , T_{22} , and T_{23} populations for ginger samples with and without CM treatment during drying

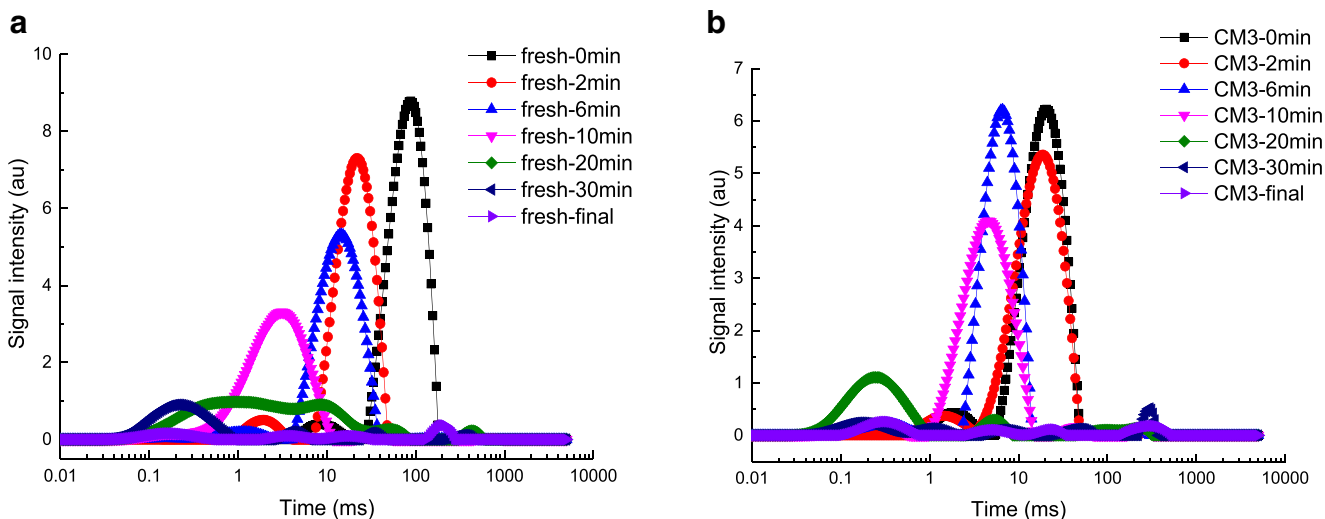


Fig. 2 Typical distribution of T_2 relaxation during vacuum microwave drying of fresh (a) and CM pretreated (b) ginger slices

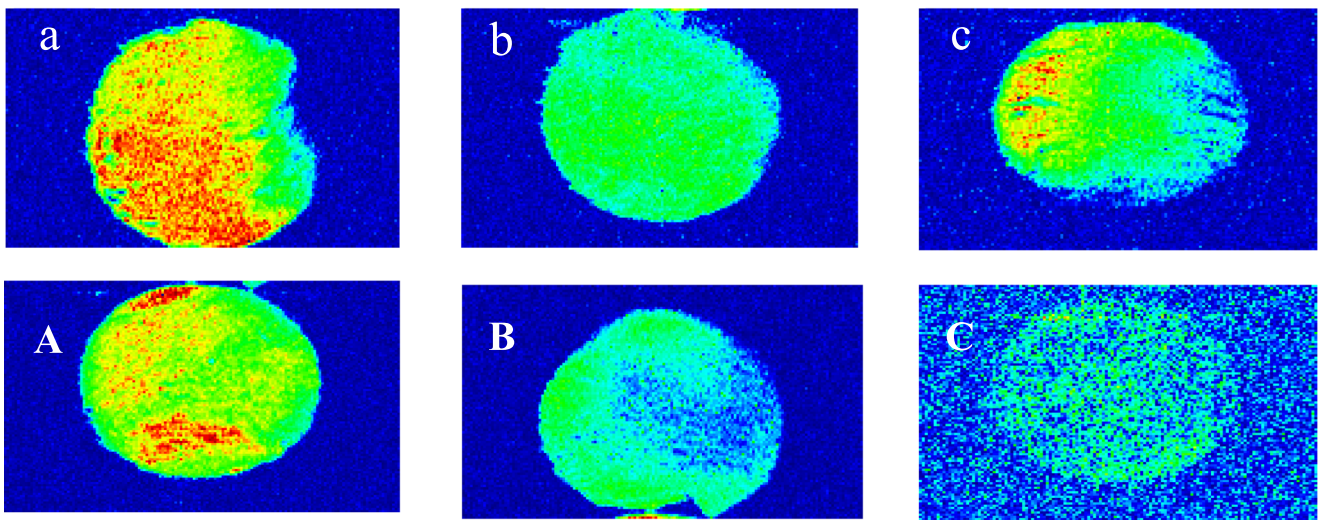


Fig. 3 Water-selective transverse images of fresh and CM pretreated ginger slices. Three images in the same row show the three different time during vacuum microwave drying of ginger with and without CM

treatment: (a) fresh 0 min; (b) fresh 2 min; (c) fresh 6 min; (a) CM 0 min; (b) CM 2 min; (c) CM 6 min

were shown in Supplementary Table S4. As it was reported, the relative areas under each peak A_{21} , A_{22} , and A_{23} represent the populations of the water in cell wall water, cytoplasm and extracellular water, and vacuole water, respectively. A_{total} is the total peak areas of the three peaks. As shown in Supplementary Table S2, with the extension of drying time, A_{total} of both the directly dried samples and the CM-treated samples showed a downward trend, and the total water content of ginger slices after CM treatment was always lower than that of the directly dried ginger slices. It can be found that after CM treatment, the contents of bound water and immobilized water of ginger slices were lower than that of the directly dried samples, whereas the content of free water was significantly

increased. Therefore, CM treatment could reduce the barrier of moisture diffusion.

As shown in Fig. 3, the brighter the MRI image of ginger is, the higher the density of protons per unit volume and the water content it would have, and vice versa. Due to the weakness of resonance signals, it was difficult to image the samples after 6 min of drying. Therefore, three time durations of 0, 2, and 6 min were selected for imaging. As the drying process progressed, the MRI image of ginger slices became darker, indicating the water content was gradually reduced (Fig. 3). After drying for the same time, the MRI image of the ginger slices treated by CM was significantly darker than the directly dried ginger slices (Fig. 3 a–c), suggesting that samples with

Fig. 4 The scanning electron micrograph of dried ginger slices with and without CM pretreatments: (a) non-CM; (b) CM1; (c) CM2; (d) CM3. Magnification: $\times 200$

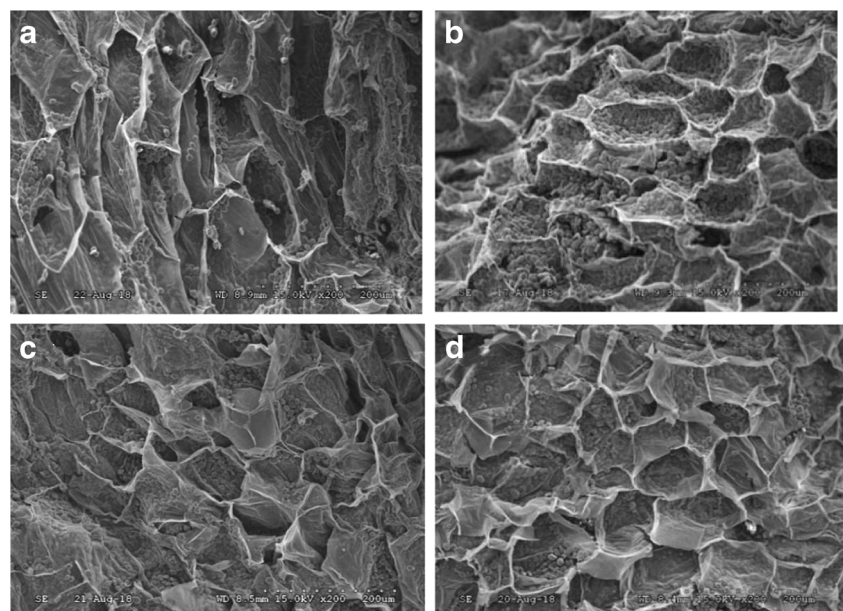


Table 1 Color of fresh and dried ginger with CM treatments

Pretreatments	L^*	a^*	b^*	ΔE
Fresh	61.74 ± 0.07^d	-8.52 ± 0.02^d	25.82 ± 0.08^d	–
Fresh + MVD	83.46 ± 0.45^c	-3.23 ± 0.01^a	34.81 ± 0.39^a	25.80 ± 0.40^a
CM1 + MVD	84.47 ± 0.21^b	-3.45 ± 0.21^a	30.18 ± 0.28^c	23.70 ± 0.17^c
CM2 + MVD	85.03 ± 0.58^a	-5.13 ± 0.06^c	33.50 ± 0.97^{ab}	24.77 ± 0.78^b
CM3 + MVD	84.97 ± 0.56^{ab}	-4.96 ± 0.48^b	31.06 ± 1.14^b	24.07 ± 0.27^b

CM treatment had higher rate of moisture diffusion and evaporation. In addition, in the ginger slices without CM treatment, the outer layer of water was removed first, whereas in the ginger slices after CM treatment, the internal and external water was removed simultaneously. This could be proved by the images in Fig. 3 a–c. Therefore, CM treatment was beneficial to improving the drying performance of ginger as well as the uniformity of samples.

Effect of CM Pretreatments on the Microstructure of Ginger Slices

As shown in Fig. 4a, parenchyma cells of dried gingers showed ambiguous contours of cell wall, turgor loss, and degradation of middle lamella. After CM pretreatment, the contours of cell wall became clear and the porous structures were produced (Fig. 4 b–d), especially for CM3 samples, whose pore structures were mostly regular and uniform. CM3 was also confirmed to show the highest drying rate among samples from other CM conditions. According to Wei et al. (2019), the pressure, temperature, and time of CM all have significant effects on the microstructure of ginger as well as drying rate. With the increase of CM pressure, temperature, and time, the pore structures were increased and enlarged, which is beneficial to the internal moisture diffusion and evaporation. But if the pressure and temperature were too high or the treatment time was too long, the CM treatment could severely damage the internal structure and reduce the diffusion rate of moisture. These findings are also consistent with the report of Liu et al. (2012) on grape.

Effect of CM Pretreatments on Quality Attributes of Dried Ginger Slices

Color

As shown in Table 1, compared with directly dried samples, samples with CM pretreatment had higher L^* values and lower a^* and b^* values, implying that the CM pretreatment could increase the lightness, and decrease the redness and yellowness of ginger. This indicated that CM could effectively reduce the enzymatic or non-enzymatic browning reaction of ginger during drying process (Krokida et al. 2008). The total color difference (ΔE) of dried gingers with CM treatment was significantly lower than that of the directly dried samples, which were closer to the color of fresh samples. Therefore, CM pretreatment can greatly help to reduce the browning reactions of ginger during drying.

6, 8, 10-gingerols, and 6-shogaol

6-gingerol, 8-gingerol, 10-gingerol, and 6-shogaol are the major pharmacologically active and pungent components of ginger (Yu et al. 2007). According to Puengphian and Sirichote (2008), gingerols consist of molecular structure of β -hydroxyl keto group that is thermally labile. The higher temperature would promote the decomposition of 6-gingerol and transformation of 6-gingerol to 6-shogaol (Huang et al. 2011). As shown in Table 2, the contents of gingerols and shogaol in ginger were significantly increased after CM treatments. Among those, CM1 (2 MPa-3 h-40 °C) had the highest

Table 2 The changes of gingerols, shogaol, and antioxidant activity of fresh and dried ginger with CM treatments

	Fresh	Fresh + MVD	CM1 + MVD	CM2 + MVD	CM3 + MVD
6-gingerol (mg/g d.w.)	29.11 ± 0.24^a	21.79 ± 0.13^d	26.32 ± 0.33^b	26.28 ± 0.11^b	24.72 ± 0.11^c
8-gingerol (mg/g d.w.)	13.87 ± 0.65^c	11.94 ± 0.41^e	16.39 ± 0.18^a	13.33 ± 0.12^d	14.45 ± 0.07^b
10-gingerol (mg/g d.w.)	10.98 ± 0.11^a	6.82 ± 0.04^e	9.33 ± 0.14^b	7.78 ± 0.10^c	7.35 ± 0.11^d
6-shogaol (mg/g d.w.)	1.36 ± 0.04^d	1.43 ± 0.01^c	2.41 ± 0.09^a	2.10 ± 0.06^b	2.36 ± 0.13^a
AEAC (mg AA/g d.w.)	1.59 ± 0.02^a	0.67 ± 0.04^e	0.89 ± 0.04^b	0.73 ± 0.03^d	0.80 ± 0.03^c
FRAP ($\mu\text{mol Vc/g d.w.}$)	102.22 ± 4.19^b	91.71 ± 1.04^d	117.12 ± 4.20^a	102.27 ± 3.47^b	96.14 ± 4.61^c
ORAC ($\mu\text{mol Trolox/g d.w.}$)	414.37 ± 1.92^a	341.75 ± 2.38^d	410.13 ± 2.56^a	371.45 ± 7.72^b	357.37 ± 2.90^c

Table 3 The activity of PPO and POD in ginger after carbonic maceration

	PPO (U/g min)	POD (U/g min)
Fresh	363.24 ± 9.14 ^a	297.64 ± 6.04 ^a
CM-1	72.15 ± 3.71 ^c	90.30 ± 8.58 ^c
CM-2	115.87 ± 8.32 ^b	119.25 ± 9.90 ^b
CM-3	87.25 ± 8.74 ^c	84.44 ± 8.84 ^c

contents of 6-gingerol, 8-gingerol, 10-gingerol, and 6-shogaol, which were increased by 20.79%, 37.27%, 36.80%, and 68.53% respectively compared with directly dried samples. In the CM pretreatments with higher temperature, such as CM2 (1 MPa-3 h-45 °C) and CM3 (2 MPa-5 h-45 °C), the gingerols and shogaol were decreased to a certain extent. This could be due to the low stability of gingerols. CM could provide an acidic environment, which is conducive to the conversion of zingerone and aldehyde to gingerols and shogaols (Bhattarai et al. 2001). However, when the temperature was higher during maceration, the gingerols and shogaols tend to converse to zingerone and corresponding aldehyde under the reaction of reverse aldol (Huang et al. 2011). Therefore, the gingerols and shogaol were decreased in CM2 and CM3. Besides, compared with CM2, the increase of maceration time in CM3 could improve the conversion of gingerols to shogaols (Table 2), which agreed with the report of Cheng et al. (2011).

The Antioxidant Activity

The antioxidant activities of ginger with and without CM treatment were evaluated using DPPH, FRAP, and ORAC

assay. The DPPH free radical is a stable free radical, which has been widely accepted as a tool for estimating the free radical scavenging activity of antioxidants. In the DPPH test, the CM pretreated gingers had significantly higher AEAC values than the directly dried samples. The highest AEAC value was observed in fresh gingers, followed by CM1, CM3, and CM2 pretreated samples, whereas the directly dried samples gave the lowest free radical scavenging ability (Table 2). The AEAC value of CM1 samples was 1.33 times of that in the directly dried samples. As shown in Table 2, after CM treatment, the FRAP values of dried gingers were significantly higher than that of the directly dried sample. The highest FRAP value observed in CM-treated samples was CM1, which was 1.28 times of that in the directly dried samples. The values of ORAC obtained in terms of Trolox equivalent showed a same trend with DPPH and FRAP assay (Table 2). The highest ORAC value was observed in CM1, which was 1.20 times of that in the directly dried samples, followed by CM2 and CM3. Therefore, CM pretreatment could be beneficial to increase the antioxidative capability of ginger after drying. Compared with samples pretreated by CM1, samples of CM2 and CM3 showed lower FRAP, AEAC, and ORAC values. This could be attributed to the higher temperature (45 °C) of CM2 and CM3. According to Huang et al. (2011), when the environment temperature is higher, the gingerols and shogaols tend to converse to zingerone and corresponding aldehyde, which presented lower antioxidant activities.

In addition, the antioxidant activities had high correlations with 6-gingerol, 8-gingerol, 10-gingerol, and 6-shogaol. The DPPH scavenging ability had positive correlations with 6-gingerol ($R^2 = 0.813$) and 10-gingerol ($R^2 = 0.919$), and negative correlation with 6-shogaol ($R^2 = -0.470$). FRAP value had all positive correlations with 6-gingerol, 8-gingerol, 10-

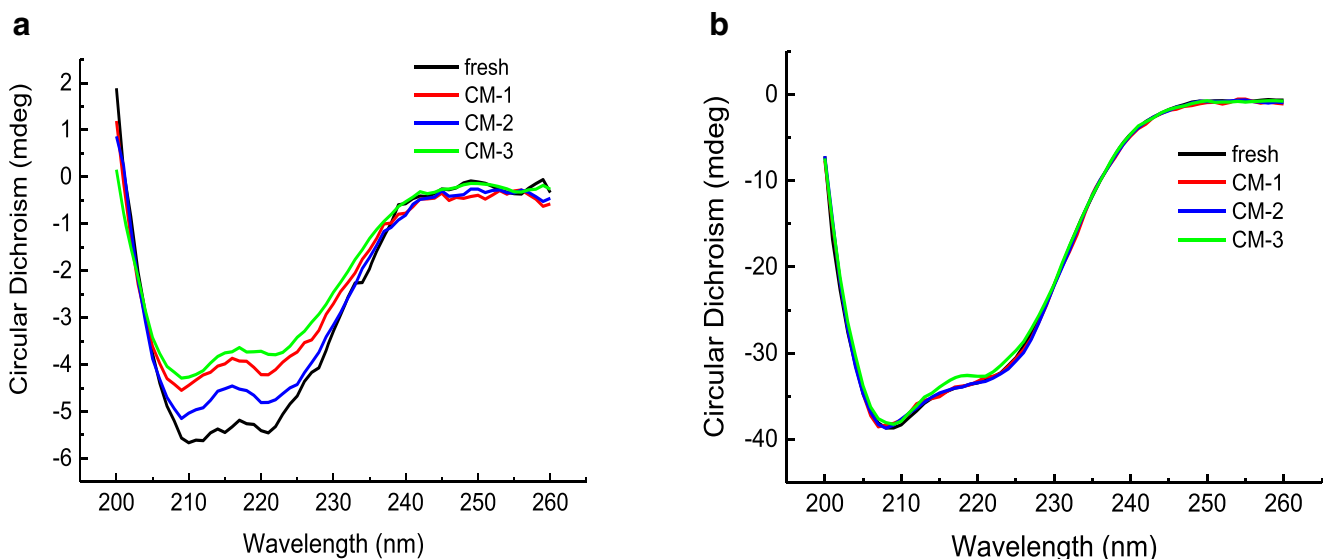


Fig. 5 Far-UV CD spectra of PPO (a) and POD (b) after CM pretreatments

Table 4 The Effects on secondary structure of PPO and POD after carbonic maceration

	CM conditions	α -helix (%)	β -sheet (%)	β -turn (%)	Rndm.coil (%)
PPO	Fresh	53.0	6.8	16.5	24.2
	CM1	45.4	11.4	18.1	26.9
	CM2	49.2	7.5	17.1	28.4
	CM3	40.5	12.6	18.5	29.1
POD	Fresh	87.2	0.2	6.2	20.1
	CM1	81.3	2.4	9.3	21.7
	CM2	83.8	1.8	7.6	20.1
	CM3	84.2	0.5	8.3	21.4

gingerol, and 6-shogaol, among which 8-gingerol showed the highest correlation ($R^2 = 0.870$). ABTS value also presented high positive correlations with 6-gingerol ($R^2 = 0.880$) and 10-gingerol ($R^2 = 0.947$).

The Effect Mechanism of CM Pretreatments

Inactivation of PPO and POD

PPO and POD are the main enzymes responsible for quality loss due to phenolic degradation. As shown in Table 3, the activities of PPO and POD were decreased significantly after all CM treatments. The activity of PPO was reduced most after treated by CM1, which was decreased by 80.14% compared with fresh samples. The activity of POD was decreased by 71.63% to the best under the treatment of CM3. Therefore, CM conditions presented different inactivation ability to PPO and POD. This may be because CO_2 penetrated into the different folding sites of enzymes, causing different changes of enzyme conformation. The inactivation of CM to the oxidizing enzymes further explained that CM helped to reduce the

browning reactions of dried ginger and increase the retention of active compounds.

Conformational Changes of PPO and POD by CM

CD Spectra Analysis CD is a valuable spectroscopic technique for studying protein conformation because common conformational motifs in protein solution contain α -helices, β -pleated sheets, poly-L-proline II-like helices, and turns. They have characteristic far UV CD spectra which directly characterize the change of protein secondary conformation (Greenfield 1999). Two negative peaks at 208 and 222 nm are characteristic of the α -helices secondary conformation of proteins, and their intensity reflects the amount of helical structure in protein. As shown in Fig. 5, PPO and POD both have double negative peaks in far UV CD spectra at around 208 and 222 nm. After CM treatment, the intensity of peaks at 208 and 222 nm was decreased significantly, indicating losses of α -helix conformation in PPO and POD (Fig. 5 a, b). As shown in Table 4, after CM treatment, the relative contents of α -helix of PPO and POD were decreased from 7.17 to

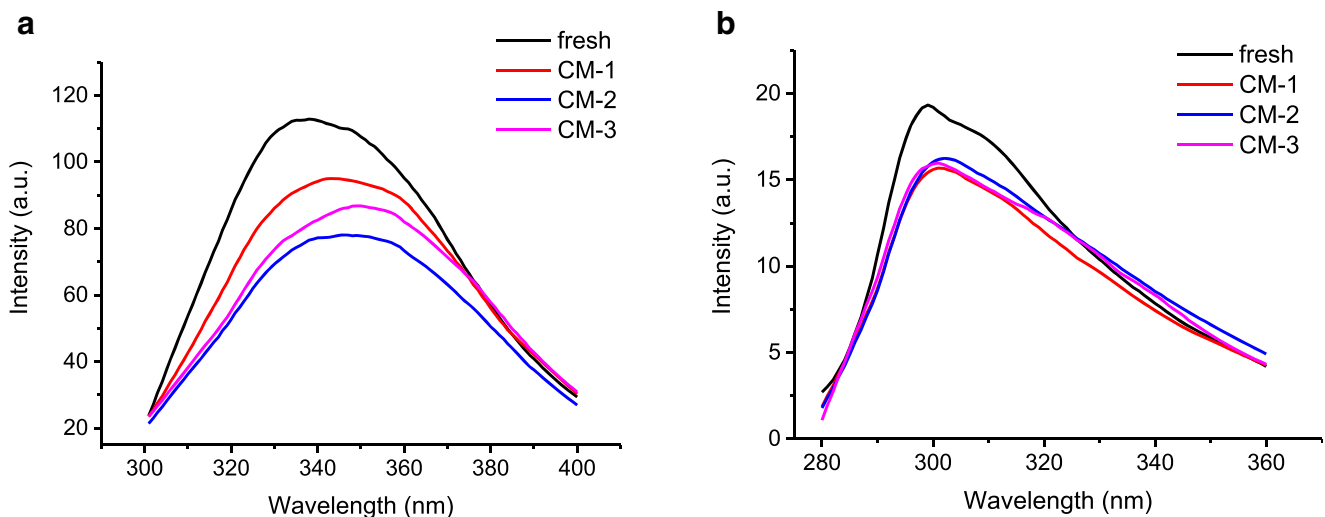
**Fig. 6** Fluorescence spectrum of PPO (a) and POD (b) after CM pretreatments

Table 5 Effects on emission wavelength and fluorescence intensity of PPO and POD after carbonic maceration

CM conditions	PPO		POD	
	Maximum emission wavelength (nm)	Relative fluorescence intensity (%)	Maximum emission wavelength (nm)	Relative fluorescence intensity (%)
Fresh	339.67 ± 2.52 ^a	100 ^a	298.40 ± 1.15 ^b	100 ^a
CM1	343.07 ± 2.00 ^a	61.60 ± 3.26 ^b	301.97 ± 1.02 ^a	59.14 ± 3.28 ^d
CM2	349.69 ± 3.23 ^b	41.62 ± 1.77 ^d	302.34 ± 1.59 ^a	69.10 ± 1.91 ^c
CM3	352.36 ± 1.50 ^b	47.51 ± 1.05 ^c	300.68 ± 1.17 ^{ab}	80.30 ± 3.64 ^b

Values with different superscript Roman letters (a–d) in the same row are significantly different according to the Duncan test ($P < 0.05$)

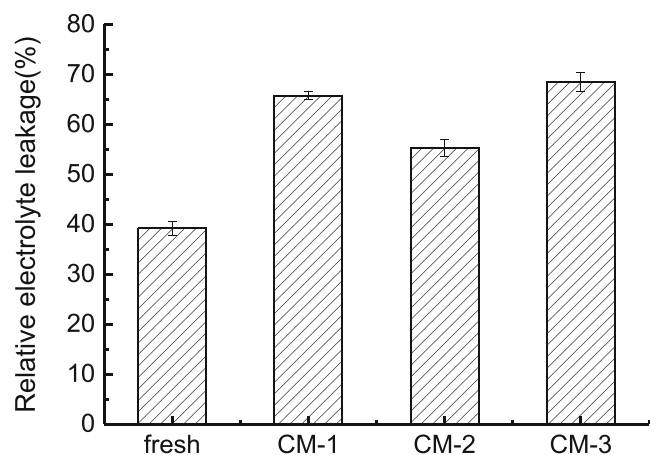
23.58% and 3.44 to 6.77%, respectively. However, the contents of β -sheet, β -turn, and random coil were increased correspondingly. This was consistent with many previous studies (Guo et al. 2017; Wimmer and Zarevúcka 2010). In the CM process, CO₂ might penetrate into the folding site of enzyme structure and interact with their protein strands and binding site to form a carbonated complex, which could cause the unfolding of α -helix to occur simultaneously with the folding of β -sheet, β -turn, and random coil. Therefore, the changes in enzyme conformation lead to the active site loss in their functions. Besides, we also found that POD had less changes in the intensity of peaks than PPO after CM treatment, indicating POD had more stable structure than PPO during carbonic maceration.

Fluorescence Spectrum Analysis Fluorescence spectroscopy is an effective method for studying the local tertiary structure of proteins. Intrinsic fluorescence of protein is due to the existence of Trp, Tyr, and Phe in protein (Zhang et al. 2006). The fluorescence spectra of PPO and POD after CM treatment were shown in Fig. 6. It should be noted that the CM treatment caused a decline in relative fluorescence intensity (Fig. 6 a and b). After CM treatment, the relative fluorescence intensities of PPO and POD were decreased by 38.4–58.38% and 19.7–

40.86%, respectively and the minimum relative fluorescence intensities for PPO and POD were 41.62% and 59.14%. Besides, the maximum emission wavelengths of PPO and POD showed substantial increase after CM pretreatments that was red shift. As shown in Fig. 6 and Table 5, the maximum red shift of PPO was from 339.67 nm (untreated) to 352.36 nm (CM3), whereas that of POD was from 298.40 nm (untreated) to 302.34 nm (CM2).

Trp, Tyr, and Phe have different fluorescence spectra because of their different side chain chromogenic groups. Trp has the highest fluorescence intensity, while Phe has a very low fluorescence intensity. It is likely that the CM-induced modification of PPO and POD conformation in the vicinity of the Trp and Tyr residues contributed to the changes in fluorescence spectra, the relative fluorescence intensity, and the red shift. It is well known that the fluorescence intensity of Trp and Tyr is quenched by polar solvent (Lakowicz 2006). When treated by carbon dioxide under certain pressure and temperature, it was possible that the enzyme was partially unfolded so that Trp and Tyr were more or less exposed to the acid environment. More chances were thus given to Trp and Tyr to contact with polar solvent. Consequently, quenching of fluorescence occurred.

Fig. 7 Changes of cell permeability of ginger after carbonic maceration



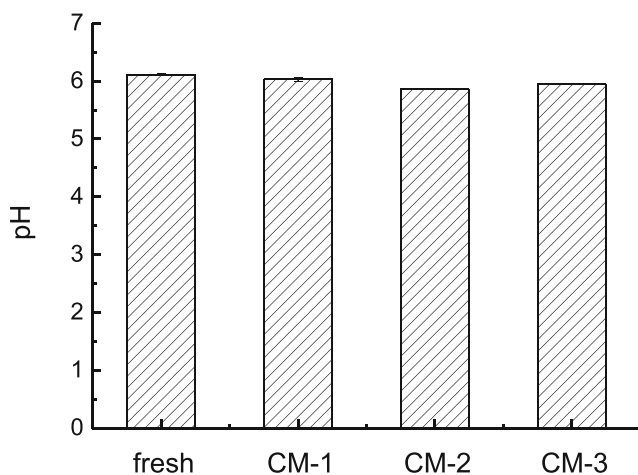


Fig. 8 Changes of intracellular pH of ginger after carbonic maceration

Changes of Cell Permeability

Cell membrane permeability of ginger slices was expressed by the change of relative electrolyte leakage (REL). The higher value of REL indicated the higher permeability of cell membrane. As shown in Fig. 7, the REL of fresh ginger was 39.26%. After CM treatment, the RELs of all samples were increased. The highest REL was 68.60%, which was 1.75 times of that for fresh. According to Parrish and Leopold (1978), when structure and function of cell membrane were disturbed, the decrease in cell membrane activity and increase in membrane permeability were observed. It suggested that CM pretreatment could cause damage to the cell structure of ginger, thus increased the membrane permeability. The increase of cell membrane permeability could considerably reduce the mass transfer resistance, improve drying efficiency, and enhance the extraction performance of active compounds (Krall and McFeeters 1998; Femenia et al. 1998).

Intracellular pH of Ginger Tissue

The changes of intracellular pH of ginger were shown in Fig. 8. The intracellular pH of fresh ginger was 6.09, and after CM treatments, the intracellular pHs of ginger were decreased by 0.99–3.78%. According to previous study (Alinia et al. 2010), the lower pH could play an important role in quality attributes.

The lower pH could enhance the hydrolysis of cellulose, yield more reducing sugar, and enhance the extraction of the TPC and antioxidant capacity. Besides, the acid environment is favorable for the stability of phenol compounds (Ruenroengkin et al. 2008).

Changes of Total Phenols, Free Phenols, and Bound Phenols

As shown in Table 6, after drying, the contents of total, free, and bound phenols of ginger were significantly decreased. However, after CM treatment, the contents of those three kinds of phenols showed significant increased, especially the free phenols, which were even higher than those in fresh ginger. The highest contents of total, free, and bound phenols occurred in CM1 treatment, which were increased by 44.07%, 256.65%, and 38.42% respectively compared with the directly dried samples. The reason for this may be because CM treatment can provide ginger with acid environment, which helped to improve the stability of phenols, and promoted the hydrolysis of bound phenols to free phenols. Furthermore, according to Que et al. (2008), the destruction of cell wall, cell membrane, and vacuole membrane could make the precursors of phenols and related enzymes more accessible, leading to the formation of new phenol compounds.

Conclusion

CM technique presented in our study is a favorable pretreatment for drying of ginger. It could help to reduce the mass transfer resistance, and increase the internal moisture diffusion and evaporation of plant material. Gingers pretreated by CM3 (2 MPa-5 h-45 °C) showed the highest drying rate, whose drying time was 42.27% less than the untreated samples. CM treatment can also enhance the extraction of active components and inactivated oxidase enzymes and improve the stability of phenolic compounds. Samples pretreated by CM1 (2 MPa-3 h-40 °C) showed the highest contents of 6-gingerol, 8-gingerol, 10-gingerol, and 6-shogaol as well as the highest antioxidant activities in FRAP, AEAC, and ORAC assay. Therefore,

Table 6 The contents of total phenol, free phenol, and bound phenol in ginger under different carbonic maceration conditions

	Total phenols (mg/g d.w.)	Free phenols (mg/g d.w.)	Bound phenols (mg/g d.w.)
Fresh	17.69 ± 0.20 ^a	5.10 ± 0.12 ^d	12.08 ± 0.06 ^a
Fresh + MVD	8.85 ± 0.28 ^e	2.03 ± 0.42 ^e	3.67 ± 0.05 ^c
CM1 + MVD	12.75 ± 0.13 ^b	7.24 ± 0.02 ^a	5.08 ± 0.10 ^b
CM2 + MVD	11.06 ± 0.01 ^d	6.48 ± 0.07 ^b	3.04 ± 0.05 ^d
CM3 + MVD	11.64 ± 0.11 ^c	6.12 ± 0.03 ^c	5.01 ± 0.06 ^b

Values with different superscript Roman letters (a–d) in the same row are significantly different according to the Duncan test ($P < 0.05$)

CM1 and CM2 are better selection of CM treatment for improving drying characteristics and preserving nutritional values and CM combined with vacuum microwave drying is a promising technology for ginger drying.

Funding Information We received financial support from the Guangzhou Science and Technology Project (201906010097); Guangzhou rural science and technology special commissioner project (GZKTP201809); National Key Research Project of China (2017YFD0400900, 2017YFD0400904); Guangdong Provincial Agricultural Science and Technology Innovation and Extension Project in 2019 (No. 2019KJ101) and CSC scholarship (File No. 201808440029).

References

- Alinia, R., Zabihi, S., Esmailzadeh, F., & Kalajahi, F. (2010). Pretreatment of wheat straw by supercritical CO₂ and its enzymatic hydrolysis for sugar production. *Biosystems Engineering*, 107(1), 61–66.
- Azzouz, S., Guizani, A., Jomaa, W., & Belghith, A. (2002). Moisture diffusivity and drying kinetic equation of convective drying of grapes. *Journal of Food Engineering*, 55(4), 323–330.
- Bain, J. M., & McBean, D. M. (1969). The development of the cuticular wax layer in prune plums and the changes occurring in it during drying. *Australian Journal of Biological Sciences*, 22(1), 101–110.
- Bhattarai, S., Tran, V. H., & Duke, C. C. (2001). The stability of gingerol and shogaol in aqueous solutions. *Journal of Pharmaceutical Sciences*, 90(10), 1658–1664.
- Chan, E. W. C., Lim, Y. Y., Wong, L. F., Lianto, F. S., Wong, S. K., Lim, K. K., Joe, T. Y., & Lim, T. Y. (2008). Antioxidant and tyrosinase inhibition properties of leaves and rhizomes of ginger species. *Food Chemistry*, 109(3), 477–483.
- Cheng, X. L., Liu, Q., Peng, Y. B., Qi, L. W., & Li, P. (2011). Steamed ginger (*Zingiber officinale*): changed chemical profile and increased anticancer potential. *Food Chemistry*, 129(4), 1785–1792.
- Chong, C. H., Figiel, A., Law, C. L., & Wojdyło, A. (2013). Combined drying of apple cubes by using of heat pump, vacuum-microwave, and intermittent techniques. *Food and Bioprocess Technology*, 7(4), 975–989.
- Doymaz, I. (2006). Drying kinetics of black grapes treated with different solutions. *Journal of Food Engineering*, 76(2), 212–217.
- Doymaz, I. (2007). Air drying characteristics of tomatoes. *Journal of Food Engineering*, 78(4), 1291–1297.
- Esturk, O. (2012). Intermittent and continuous microwave-convective air-drying characteristics of Sage (*Salvia officinalis*) leaves. *Food and Bioprocess Technology*, 5(5), 1664–1673.
- Femenia, A., Sanchez, E. S., Simal, S., & Rossello, C. (1998). Effects of drying pre-treatments on the cell wall composition of grape tissues. *Journal of Agricultural and Food Chemistry*, 46, 271–276, 1.
- Figie, A. (2009). Drying kinetics and quality of vacuum-microwave dehydrated garlic cloves and slices. *Journal of Food Engineering*, 94(1), 98–104.
- Figie, A. (2010). Drying kinetics and quality of beetroots dehydrated by combination of convective and vacuum-microwave methods. *Journal of Food Engineering*, 98(4), 461–470.
- Galindo, F. G., Toledo, R. T., & Sjöholm, I. (2005). Tissue damage in heated carrot slices: comparing mild hot water blanching and infra-red heating. *Journal of Food Engineering*, 67(4), 381–385.
- Greenfield, N. J. (1999). Applications of circular dichroism in protein and peptide analysis. *Trends in Analytical Chemistry*, 18(4), 236–244.
- Guo, J., Wu, H., Du, L., Zhang, W., & Yang, J. (2014). Comparative antioxidant properties of some gingerols and shogaols, and the relationship of their contents with the antioxidant potencies of fresh and dried ginger (*Zingiber officinale* Roscoe). *Journal of Agricultural Science and Technology*, 16(5), 1063–1072.
- Guo, M. H., Liu, S. C., Ismail, M., Farid, M. M., Ji, H. W., Mao, W. J., et al. (2017). Changes in the myosin secondary structure and shrimp surimi gel strength induced by dense phase carbon dioxide. *Food Chemistry*, 227, 219–226.
- Huang, T. C., Chung, C. C., Wang, H. Y., Law, C. L., & Chen, H. H. (2011). Formation of 6-shogaol of ginger oil under different drying conditions. *Drying Technology*, 29(16), 1884–1889.
- Krall, S. M., & McFeeters, R. F. (1998). Pectin hydrolysis: effect of temperature, degree of methylation, pH and calcium on hydrolysis rates. *Journal of Agricultural and Food Chemistry*, 46(4), 1311–1315.
- Krokida, M. K., Maroulis, Z. B., & Saravacos, G. D. (2008). The effect of the method of drying on the colour of dehydrated products. *International Journal of Food Science and Technology*, 36(1), 53–59.
- Lakowicz, J. R. (2006). *Quenching of fluorescence. Principles of fluorescence spectroscopy* (pp. 278–327). Germany: Springer.
- Larsen, K., Ibrahim, H., Khaw, S. H., & Saw, L. G. (1999). Gingers of Peninsular Malaysia and Singapore. *Singapore: Natural history publications* (Borneo), pp. 135.
- Lim, Y. Y., & Murtijaya, J. (2007). Antioxidant properties of Phyllanthus amarus extracts as affected by different drying methods. *LWT- Food Science and Technology*, 40(9), 1664–1669.
- Liu, L. J., Wang, Y. X., Zhao, D. D., An, K. J., Ding, S. H., & Wang, Z. F. (2014). Effect of carbonic maceration pre-treatment on drying kinetics of chili (*Capsicum annuum* L.) flesh and quality of dried product. *Food and Bioprocess Technology*, 7(9), 2516–2527.
- Liu, M. Y., Guo, Y. H., Zhao, C. P., & Wang, Z. F. (2012). Optimization of drying and fermentation process for carbon dioxide assisted fermentation. *Transactions of the Chinese Society of Agricultural Engineering*, 28(12), 269–272.
- Liu, M. Y., & Wang, Z. F. (2011). Effect of carbon dioxide fermented condition on compositions of grapes. *China Brewing (in Chinese)*, 235(10), 142–144.
- Mishra, B. B., Gauta, S., & Sharma, A. (2004). Shelf-life extension of fresh ginger (*Zingiber officinale*) by gamma irradiation. *Journal of Food Science*, 69(9), 274–279.
- Parrish, D. J., & Leopold, C. A. (1978). On the mechanism of aging in soybean seeds. *Plant Physiology*, 61(3), 365–368.
- Puengphian, C., & Sirichote, A. (2008). [6]-Gingerol content and bioactive properties of ginger (*Zingiber officinale* Roscoe) extracts from supercritical CO₂ extraction. *Asian Journal of Food and Agro-Industry*, 1(1), 29–36.
- Que, F., Mao, L. C., Fang, X. H., & Wu, T. (2008). Comparison of hot-air drying and freeze-drying on the physicochemical properties and antioxidant activities of pumpkin (*Cucurbita moschata* Duch.) flours. *International Journal of Food Science and Technology*, 43(7), 1195–1201.
- Romano, G., Baranyai, L., Gottschalk, K., & Zude, M. (2008). An approach for monitoring the moisture content changes of drying banana slices with laser light backscattering imaging. *Food and Bioprocess Technology*, 1(4), 410–414.
- Ruenroengkin, N., Zhong, J., & Jiang, Y. M. (2008). Effect of various temperatures and pH values on the extraction yield of phenolics from litchi fruit pericarp tissue and the antioxidant activity of the extracted anthocyanins. *International of Molecular Science*, 9(7), 1333–1341.
- Shukla, Y., & Singh, M. (2007). Cancer preventive properties of ginger: a brief review. *Food and Chemical Toxicology*, 45(5), 683–690.

- Singleton, V., Orthofer, R., & Lamuela-Raventos, R. (1999). Analysis of total phenols and other oxidation substrates and antioxidants by means of Folin-Ciocalteu reagent. Oxidants and antioxidants part A. *Methods in Enzymology*, 299, 152–178.
- Taiwo, K. A., Angersbach, A., & Knorr, D. (2002). Influence of high intensity electric field pulses and osmotic dehydration on the rehydration characteristics of apple slices at different temperatures. *Journal of Food Engineering*, 52(2), 185–192.
- Tao, H.Y. (2013). Effect of different pretreatments on drying characteristics and product quality of red grapes. [Master's Thesis] Beijing: China Agricultural University.
- Tarhan, S. (2007). Selection of chemical and thermal pretreatment combination for plum drying at low and moderate drying air temperatures. *Journal of Food Engineering*, 79(1), 255–260.
- Tesniere, C., & Flanzy, C. (2011). Carbonic maceration wines: characteristics and winemaking process. *Advances in Food and Nutrition Research*, 63, 1–15.
- Thakor, N. J., Sokhansanj, S., Sosulski, F. W., & Yannacopoulos, S. (1999). Mass and dimensional changes of single canola kernels during drying. *Journal of Food Engineering*, 40(3), 153–160.
- Turgut, S.S., Yanik, M. M., Karacabey, E., & Kucukoner, E. (2018). Effect of carbonic maceration pre-treatment on quality characteristics of French fries and a numerical approach for prediction of moisture and temperature distribution. *International Journal of Food Engineering*, 4(3), 170–177.
- Wang, L., Xu, B., Wei, B., & Zeng, R. (2018). Low frequency ultrasound pretreatment of carrot slices: effect on the moisture migration and quality attributes by intermediate-wave infrared radiation drying. *Ultrasonics Sonochemistry*, 40(Pt A), 619–628.
- Wei, L., Wang, Z. T., Yu, Y. S., Xu, Y. J., & An, K. J. (2019). Effect of carbonic maceration treatment on vacuum-microwave drying characteristics and microstructure of ginger. *Modern Food Science and Technology*, 35(8), 121–129.
- Wimmer, Z., & Zarevúcka, M. (2010). A review on the effect of supercritical carbon dioxide on enzyme activity. *International Journal of Molecular Sciences*, 11(1), 233–253.
- Wolfe, K. L., Kang, X., He, X., Dong, M., Zhang, Q., & Liu, R. H. (2008). Cellular antioxidant activity of common fruits. *Journal of Agricultural and Food Chemistry*, 56(18), 8418–8426.
- Xu, B. G., Zhang, M., Bhandari, B., Cheng, X. F., & Sun, J. (2015). Effect of ultrasound immersion freezing on the quality attributes and water distributions of wrapped red radish. *Food and Bioprocess Technology*, 8(6), 1366–1376.
- Yu, Y., Huang, T., Yang, B., Liu, X., & Duan, G. (2007). Development of gas chromatography–mass spectrometry with microwave distillation and simultaneous solid-phase micro-extraction for rapid determination of volatile constituents in ginger. *Journal of Pharmaceutical and Biomedical Analysis*, 43(1), 24–31.
- Zhang, R., Cheng, L., Wang, L., & Guan, Z. (2006). Inactivation effects of PEF on horseradish peroxidase (HRP) and pectinesterase (PE). *IEEE Transactions on Plasma Science*, 34(6), 2630–2636.

Publisher's Note Springer Nature remains neutral with regard to jurisdictional claims in published maps and institutional affiliations.